WILEY-VCH

Supporting Information

Flexible confinement and manipulation of Mie resonances via nano rectangular hollow metasurfaces

Zhancheng Li, Guangzhou Geng, Jiaqi Cheng, Wenwei Liu, Shiwang Yu, Boyang Xie*, Hua Cheng*, Junjie Li*, Wenyuan Zhou, Jianguo Tian, Shuqi Chen*

Dr. Z. Li, Dr. G. Geng, Dr. J. Cheng, Dr. W. Liu, Dr. S. Yu, Dr. B. Xie, Prof. H. Cheng, Prof. W. Zhou, Prof. J. Tian, Prof. S. Chen
The Key Laboratory of Weak Light Nonlinear Photonics, Ministry of Education, Renewable Energy Conversion and Storage Center, School of Physics and TEDA Institute of Applied Physics, Nankai University, Tianjin 300071, China
E-mail: byxie@nankai.edu.cn; hcheng@nankai.edu.cn; schen@nankai.edu.cn
Prof. J. Li
Beijing National Laboratory for Condensed Matter Physics, Institute of Physics, Chinese Academy of Sciences, Beijing 100190, China
E-mail: jjli@iphy.ac.cn
Prof. S. Chen
The Collaborative Innovation Center of Extreme Optics, Shanxi University, Taiyuan, Shanxi 030006, China
Collaborative Innovation Center of Light Manipulations and Applications, Shandong Normal University, Jinan 250358, China

This file includes:

S1. Robustness of the optical responses of the designed Nano Rectangular Hollow (NRH) metasurfaces to the incident angle

S2. Analysis on the principle of the frequency-domain confinement of Mie-resonance in the designed NRH metasurfaces

S3. Advantages of NRH metasurfaces for the realization of frequency-selective optical encryption

S4. Manipulating the resonant wavelength of the proposed NRH metasurfaces in the whole visible spectrum

S5. Comparison between the simulated and measured transmission spectra of NRH metasurfaces with different lengths l

S6. The permittivity of TiO_2 used in numerical simulation

S1. Robustness of the optical responses of the designed NRH metasurfaces to the incident angle

We investigate the robustness of the optical responses of the designed NRH metasurfaces to the incident angles, as shown in **Figure S1**. The optical responses of the designed NRH metasurface remains almost unchanged under the TE illumination, while it is very sensitive to the change of the incident angle under the TM illumination. This is predictable because the resonance is mainly attributed to the magnetic dipole, as illustrates in Figure 3e.
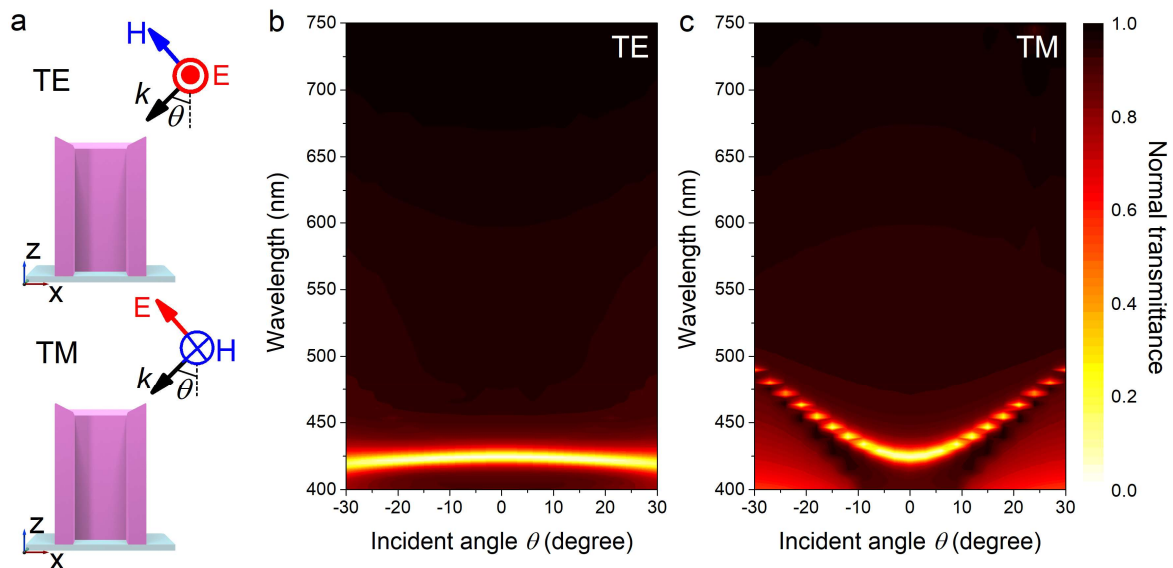
Figure S1. (a) Schematic of the TE and TM illumination condition. Simulated results of the transmission spectra as a function of incident angle under (b)TE and (c)TM illuminations. The structural parameters of the NRH metasurfaces are $l = 160$ nm, $S = 80$ nm and $t = (t_0+40)$ nm.

S2. Analysis on the principle of the frequency-domain confinement of Mie-resonance in the designed NRH metasurfaces

The Mie-resonance in the design NRH metasurfaces can be confined in a narrow bandwidth when compared with that of the nanoblock metasurfaces, which is mainly attributed to the change of the refractive index in the nano hollow. As shown in Figure 3a and 3b, the resonant

modes in the NRH and nanoblock metasurfaces are similar. However, the resonant strength of the NRH metasurfaces decreases faster than that of the nanoblock metasurfaces with the change of wavelength because the displacement currents are constrained in the thin TiO_2 structure, as shown in Figure 3c to 3e. The excitations of the electric quadrupole and the magnetic dipole are validated with the simulated results in **Figure S2**.

Figure 2c indicates that the resonance at the short wavelength, which is attributed to the electric quadrupole mode, is gradually suppressed with the increase of the diameter of the nano hollow, resulting in the confinement of the resonance in the frequency domain. This is mainly attributed to the change of the refractive index in the nano hollow, since the displacement currents in the short wavelengths are mainly excited in the centre of the nanoblocks. To further validated our claim, we simulated the electric field amplitude distribution in the *x-z* plane at different wavelengths in the nanoblock metasurfaces, as shown in **Figure S3**. The results prove that the displacement currents at the long wavelength (440 nm) are mainly excited in the edge of the nanoblocks, while them at the short wavelengths (410 nm and 420 nm) are mainly excited in the centre of the nanoblocks. The resonance will be suppressed instead of be confined in the frequency domain for dielectric metasurfaces in which the Mie-resonance-induced displacement currents are mainly excited in the centre of the nanoblocks. Therefore, the proposed NRH metasurfaces provide an effective approach for the frequency-domain confinement of Mie-resonance, which can be used to realize a transmission valley with a narrow bandwidth. A comprehensive comparison between the proposed NRH metasurfaces and the previous designs for the implementation of Mie resonances with narrow resonant bandwidth is presented in **Table S1**.
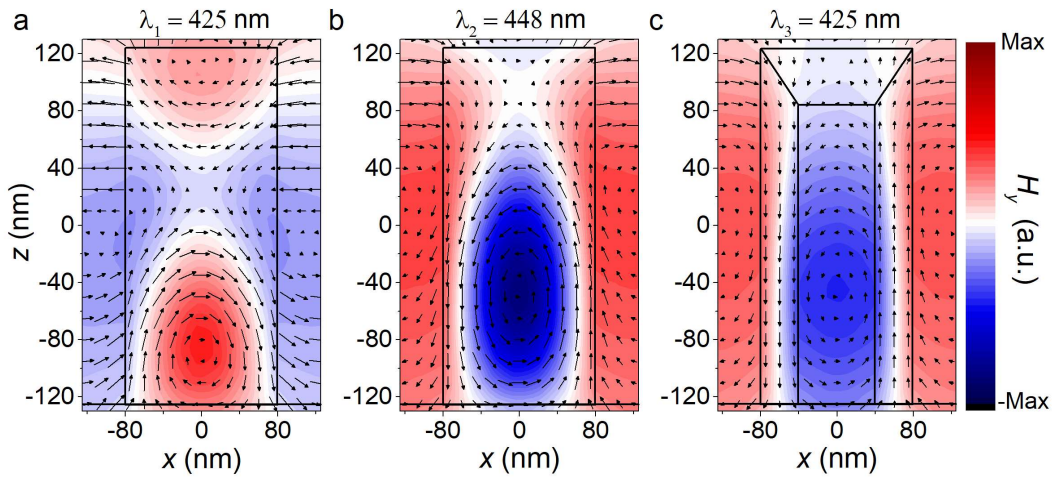
Figure S2. Simulated results of the electric field flows (black arrows) and the magnetic field (*y*-component) distribution in the *x-z* plane (*y* = 0 nm) at (c) λ_1 = 425 nm, (d) λ_2 = 448 nm for the nanoblock metasurface and at (e) λ_3 = 425 nm for the NRH metasurface.
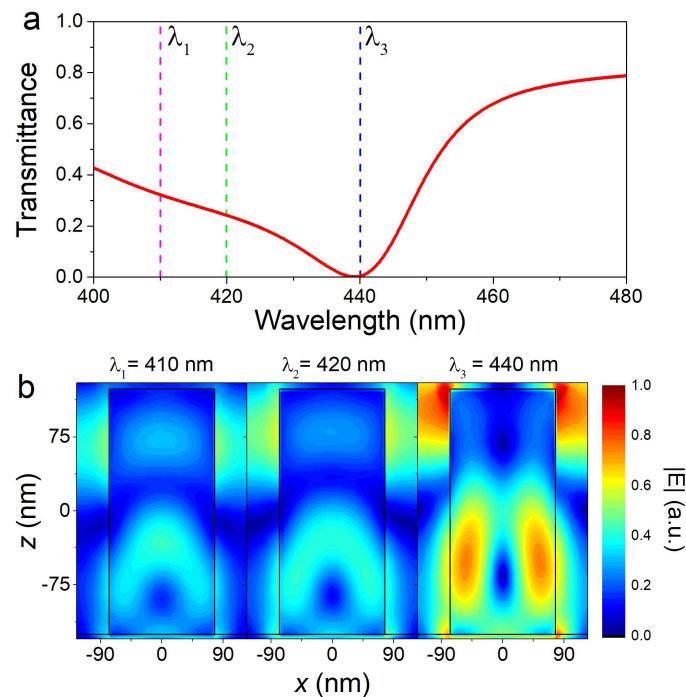

Figure S3. (a) Simulated transmission spectrum of a TiO_2 dielectric metasurface composed of nanoblocks with *l* = 160 nm, *t* = 250 nm and *p* = 250 nm. (b) Simulated results of the electric field amplitude distribution in the *x-z* plane (*y* = 0 nm) at different wavelengths in the nanoblock metasurface.

Material	Structure	Operation waveband	Quality factor and the resonant wavelength	Robustness to fabrication	Application
TiO_2 [Our work]	nano rectangular hollows	400-750 nm	43.3 (424.3 nm)	good	frequency-selective intensity manipulation and optical encryption
TiO_2, SiO_2, Si_3N_4 [S1]	multi-dielectric stacked layers	400-750 nm	~16 (497 nm)	moderate	ultrahigh-saturation structural colour
TiO_2 [S2]	double elliptical cylinders	970-1070 nm	~350 (1055 nm)	moderate	spin-selective asymmetric transmission of optical waves
AlGaAs [S3]	cylinder	1500-1700 nm	~188 (1570 nm)	moderate	second harmonic generation enhancement
Si_3N_4 [S4]	nanoholes	308-328 nm	3.54×10^4 (320.85 nm)	poor	light confinement
amorphous Si [S5]	asymmetric nano bar pairs	1050-1400 nm	10^5 (1302.6 nm)	poor	refractive index sensor
single-crystalline Si [S6]	cylinder	400-750 nm	12.6 (404 nm)	good	high-performance structural colour

Table S1. A comprehensive comparison between the proposed NRH metasurfaces and the previous designs for the implementation of Mie resonances with narrow bandwidth.

S3. Advantages of NRH metasurfaces for the realization of frequency-selective optical encryption

The influence of the structural parameter l on the resonance of the NRH metasurface is shown in Figure 4. To further show the advantages of the NRH metasurface for the implementation of frequency-selective optical encryption, we make a comparison between the NRH and nanoblock metasurfaces with different lengths l. As shown in **Figure S4**a, the resonant wavelength of the nanoblock metasurface has a larger red shift with the increase of l when compared with that of the NRH metasurface. Moreover, we simulated the variation of the transmission intensity at 416 nm (the valley values of the transmission spectra when l =140 nm) for nanoblock metasurfaces with different lengths l, as shown in Figure S4b. The results indicate that the transmission intensity at 412 nm for the NRH metasurface undergoes significant change over the variation of l when compared with that of the nanoblock metasurface at 416 nm.

Specifically, as shown in Figure S4c, the color of the nanoblock metasurface will significantly change with the variation of l from 140 to 170 nm. Therefore, the NRH metasurface is a good alternative for frequency-selective optical encryption since it has a large manipulation depth of the transmission intensity at the operation wavelength and the encoded information can be hardly recognized under the white illumination.
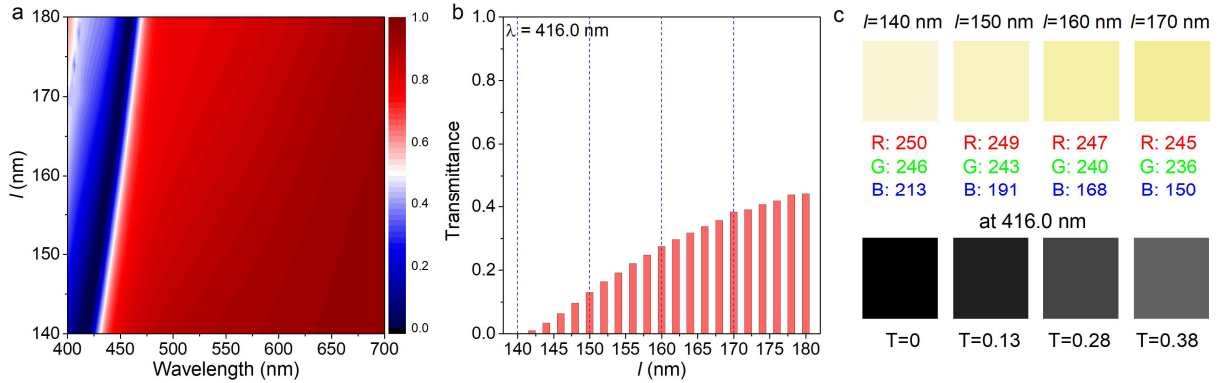

Figure S4. (a) Transmission spectra of nanoblock metasurfaces with different l. (b) Simulated transmission intensity as a function of l at 416 nm. (c) Simulated results of the color images (and the corresponding RGB values), and the gray images (and the corresponding transmission intensities) at 416 nm of periodic nanoblock metasurfaces with different l. The color images were calculated with D50 light source and the viewing angle is 10 degrees. The wavelengths 416 nm is the valley values of the transmission spectra of the nanoblock metasurface with l = 140 nm.

S4. Manipulating the resonant wavelength of the proposed NRH metasurfaces in the whole visible spectrum

The variation of the transmission spectrum of the designed NRH metasurface with the changing of structural parameters S and l has been well analyzed in Figure 2 and Figure 4, respectively. Here, we further analyze the influence of the structural parameters t_0 and P on the transmission spectrum of a designed NRH metasurface, as shown in **Figure S5**. The resonant wavelength of the designed metasurface has a red shift with the increase of the structural parameters t_0 and P,

which is in consist with the rules in dielectric metasurfaces composed of nanoblocks and

nanocylinders. The variation of t_0 changes the intrinsic optical resonance of the NRH, while the

variation of P changes the coupling between the resonance in the adjacent NRHs.

Since the resonant wavelength of the NRH metasurface has a red shift with the increase of

the structural parameters P and l, it can be further manipulated in the whole visible regime by

increasing P and l at the same time, as shown in **Figure S6**. Therefore, the NRH metasurfaces

can not only realize the flexible confinement of Mie resonances in the frequency domain, but
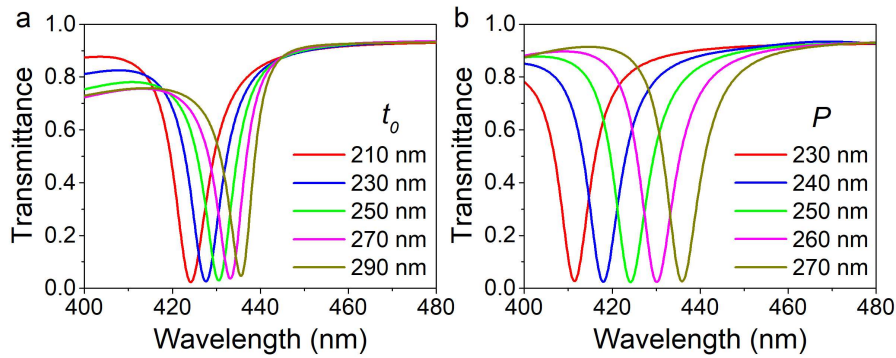
also manipulate the resonant wavelength.

Figure S5. The variation of the transmission spectrum with the changing of the structural

parameters t_0 and P for NRH metasurfaces with $l = 160$ nm, $S = 80$ nm and $t = (t_0+40)$ nm.
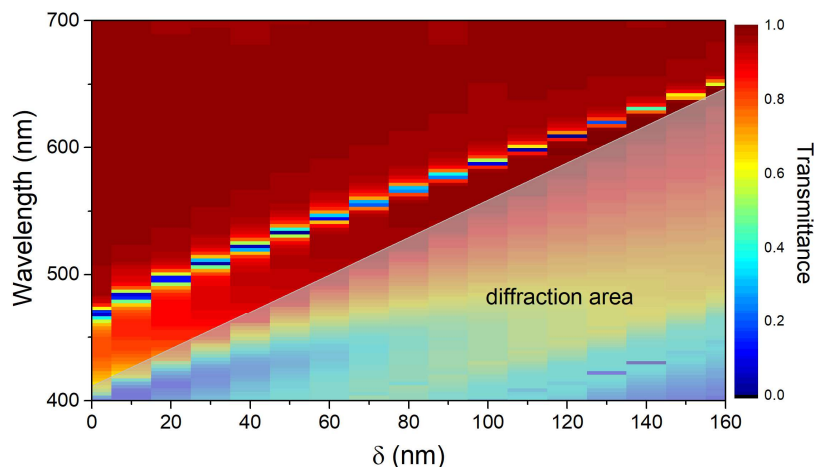

Figure S6. The variation of the transmission spectrun with the changing of the variable δ for

NRH metasurfaces with $l = (S+100)$ nm, $S = (70+\delta)$ nm, $t = (t_0+40)$ nm, $t_0 = 300$ nm, $P = (280+\delta)$

nm.

S5. Comparison between the simulated and measured transmission spectra of NRH metasurfaces with different lengths *l*

Figure S7 shows the simulated and measured transmission spectra of NRH metasurfaces with different *l*. The operation wavelengths of QR code 1 and QR code 2 in Figure 5 are designed at 410 nm (red vertical line in Figure S7a), and the operation wavelength of the 4-level gray image is designed at 430 nm (blue vertical line in Figure S7a). With the consideration of our experimental setup, we choose the wavelengths of 415 nm and 430 nm (marked by the vertical dash red line and blue line in Figure S7b) for the experimental capture of the OR code images and the gray image, respectively.
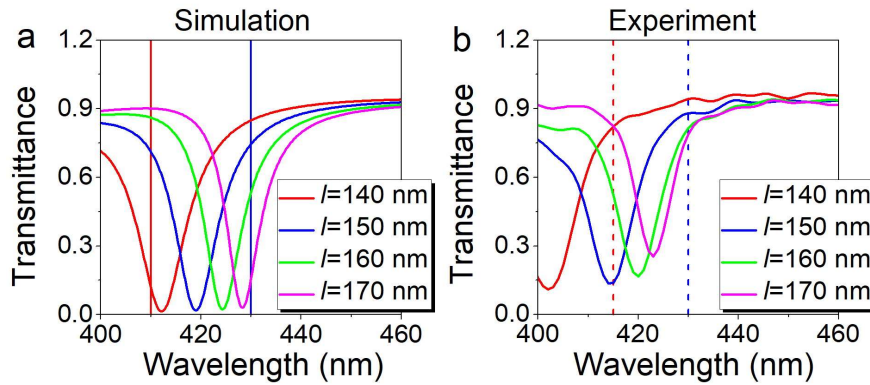

Figure S7. The (a) simulated and (b) experimental results of the transmission spectra of NRH metasurfaces with different *l*.

S6. The permittivity of TiO₂ used in numerical simulation

We choose TiO_2 as the constituent material of the NRHs because its refractive index is sufficient high in the visible regime (as shown in **Figure S8**) to support Mie resonances. Meanwhile, compared with high refractive index materials (such as Si and GaAs), the loss of TiO_2 is negligible in the visible regime. Therefore, TiO_2 is a good choice as the constituent material of dielectric metasurfaces in the visible regime.
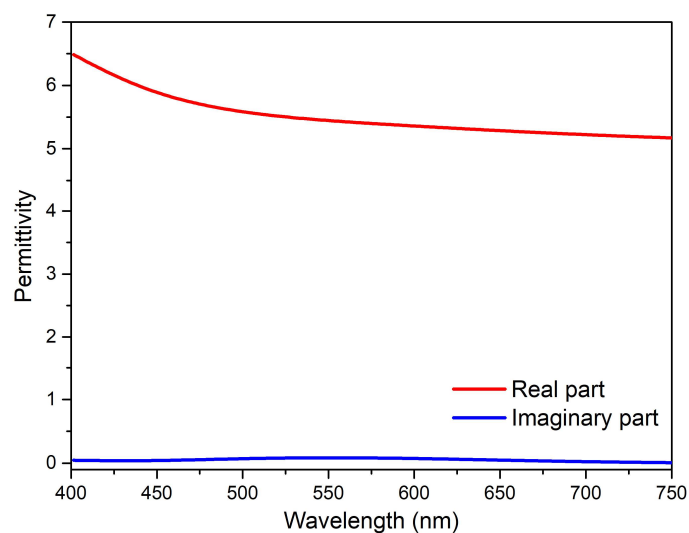
Figure S8. The permittivity of TiO$_2$ from experimentally measured data.

References

[S1] B. Yang, W. Liu, Z. Li, H. Cheng, D. Y. Choi, S. Chen, J. Tian, *Nano Lett.* **2019**, 19, 4221-4228.

[S2] D. Ma, Z. Li, Y. Zhang, W. Liu, H. Cheng, S. Chen, J. Tian, *Opt. Lett.* **2019**, 44, 3805-3808.

[S3] K. Koshelev, S. Kruk, E. Melik-Gaykazyan, J. H. Choi, A. Bogdanov, H. G. Park, Y. Kivshar, *Science* **2020**, 367, 288-292.

[S4] X. Wang, S. Li, C. Zhou, *Optics Express* **2020**, 28, 11983-11989.

[S5] Y. Zhang, W. Liu, Z. Li, Z. Li, H. Cheng, S. Chen, J. Tian, *Optics Lett.* **2018**, 43, 1842-1845.

[S6] W. Yang, S. Xiao, Q. Song, Y. Liu, Y. Wu, S. Wang, J. Yu, J. Han, D. P. Tsai, *Nature Commun.* **2020**, 11, 1864.